Journal of Engineering Sciences, Assiut University, Vol. 39 No 2 pp.359 -376 March 2011

PARAMETER OPTIMIZATION IN SPRING-ROLL DIELECTRIC ELASTOMER ACTUATOR DESIGN

Medhat H. A. Awadalla, and
Electronics and Communication Dept.,Faculty of Engineering, Helwan University, Cairo, Egypt E-mail:awadalla_medhat@yahoo.co.uk
Besada A. Anees
Industrial Training Council.,Cairo, Egypt
E-mail: bessada_adib@yahoo.com

(Received December 23, 2010 Accepted January 20, 2011)

The performance of a given type of actuators can be markedly enhanced by judicious choosing parameters of design. However, choosing parameters of design to optimize the actuator's performance has been challenging due to nonlinear equations of state, multiple modes of failure, parameters of design, and measures of performance. The actuator has three dimensionless parameters of design, the pre-stretches in length and width of the plane of the elastomer membrane and the dimensionless ratio between the stiffness of the spring and that of the elastomer. These parameters of design are prescribed once the actuator is constructed. This paper aims to optimize these parameters to get the maximum actuation of Spring-Roll Dielectric Elastomer actuator. Analysis and software programs are developed to graphically represent the equations of state for any design parameter values. Also, to design the dimensions of the actuator, the applied voltage, and the stiffness of the spring when the axial length at relax and axial load are prescribed. Different loads and actuator axial lengths and their counterpart designs are also addressed. Actuation range and maximum actuation for each design are determined. Compared with the most recent work [1-6], the achieved results show that the presented work outperforms.
In addition to, getting out of the region of failure modes is described. This paper also presents robust and reliable design techniques for a Spring-Roll Dielectric Elastomer Actuator, whose actuation exceeds 300 % and could be used as a promising device in various medical applications.

KEYWORDS: *Spring roll dielectric elastomer actuator, modes of failure, region of allowable states, actuation range, optimal design parameters.*

1. INTRODUCTION

Dielectric elastomer actuators have been intensely studied in the recent decade. To explore some of the basic issues in the design, one particular type of actuators is studied, the spring-roll actuators [7-9]. The construction of a spring-roll actuator is sketched in Fig. 1. Two membranes of a dielectric elastomer are alternated with two

electrodes. The laminate is prestretched in two directions in the plane, and then rolled around a spring [10].

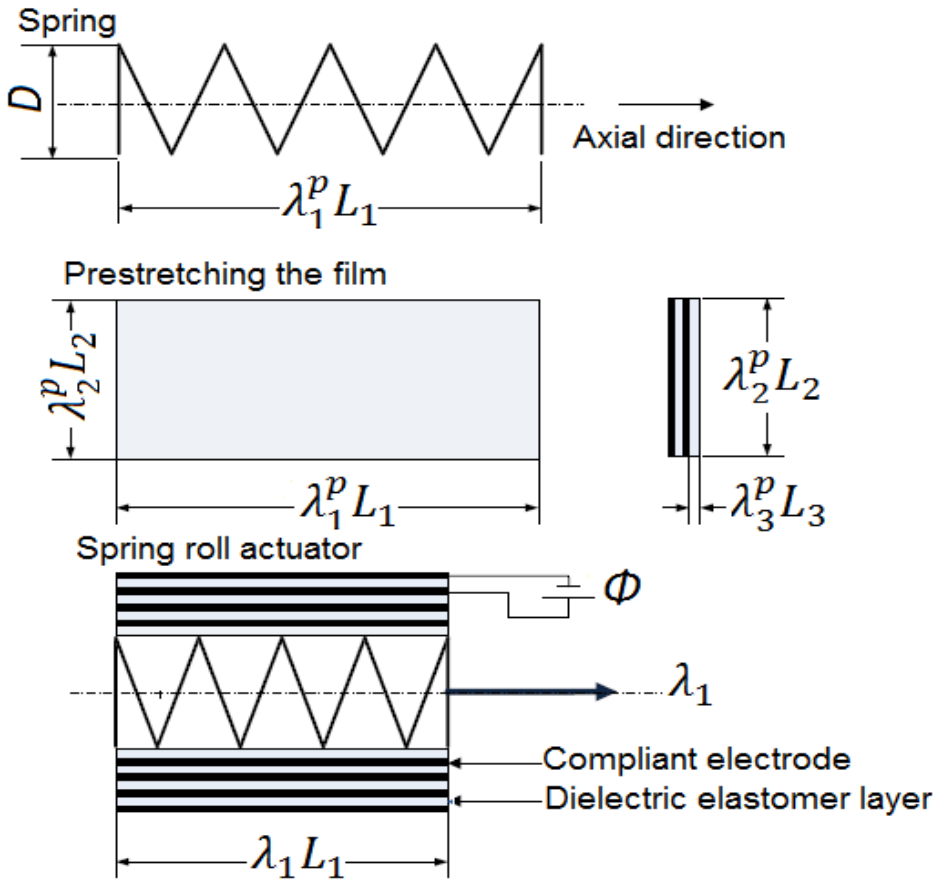

Fig. 1. The construction of a spring-roll actuator

Two membranes of a dielectric elastomer are alternated with two electrodes. The laminate is first prestretched and then rolled around a relaxed spring. When the spring roll is subject to a voltage and an axial force, the length of the spring couples the electrical and mechanical actions.

Providing dielectric elastomer actuators with a level of pre-stretch can improve properties such as breakdown strength, actuation strain and efficiency [11].

When the actuator is subjected to an applied voltage and an applied axial force, the axial elongation couples the electrical and mechanical actions. The parameters of design include prestretches of the elastomer and the stiffness of the spring.

2. EQUATIONS OF STATE

Referenced to Fig. 1, the electrodes are compliant and bear no mechanical load. The elastomer is of thickness L3 and sides L2 and L1. The relaxed spring is of length $\lambda_1^p L_1$.

The elastomer is prestretched to $\lambda_2^p L_2$ and $\lambda_1^p L_1$, and then the elastomer is rolled around the relaxed spring. When the actuator is subjected to an applied voltage Φ and an axial force P, the thickness of the laminate changes to $\lambda_3 L_3$, and the length of the spring changes to $\lambda_1 L_1$. However, side 2 of the laminate, $\lambda_2^p L_2$ is constrained by the diameter of the spring and remains unchanged. The elastomer is taken to be incompressible, so that $\lambda_1 \lambda_2^p \lambda_3 = 1$

During the operation, the actuator varies its state in two ways, as specified by two generalized coordinates: the stretch λ_1 in the axial direction, and the charge Q on one of the electrodes. Helmholtz free energy A of the actuator is prescribed as a function of the two generalized coordinates:

$$A(\lambda_1, Q) = \frac{\mu}{2}\left(\lambda_1^2 + \left(\lambda_2^p\right)^2 + \left(\lambda_1\lambda_2^p\right)^{-2} - 3\right)L_1L_2L_3 + \frac{1}{2\varepsilon}\left(\frac{Q}{\lambda_1 L_1 \lambda_2^p L_2}\right)^2 L_1L_2L_3 + \frac{1}{2}K\left(\lambda_1 L_1 - \lambda_1^p L_1\right)^2 \tag{1}$$

The free energy of the elastomer is the sum of the elastic energy, with μ being the shear modulus of the elastomer and the dielectric energy, with ε being the permittivity of the elastomer [12, 13]. The spring is taken to obey Hooke's law, with k being the stiffness of the spring.

When the actuator is in a state (λ_1, Q), in equilibrium with the applied axial force P and the applied voltage Φ, for any small change in the stretch and charge, $d\lambda_1$ and dQ, the change in the Helmholtz free energy equals the work done by the applied force and the voltage, namely [14].

$$dA = PL_1 + \Phi dQ \tag{2}$$

Consequently, the force and the voltage are the partial differential coefficients of the free-energy function $A(\lambda_1, Q)$. The axial force is work-conjugate to the elongation:

$$P = \frac{\partial A(\lambda_1, Q)}{L_1 \partial \lambda_1} \tag{3}$$

The voltage is work-conjugate to the charge:

$$\Phi = \frac{\partial A(\lambda_1, Q)}{\partial Q} \tag{4}$$

Inserting (1) into (3), we obtain that

$$\frac{P}{\mu L_2 L_3} = \left(\lambda_1 - \lambda_1^{-3}\left(\lambda_2^p\right)^{-2}\right) - \frac{1}{\lambda_1^3\left(\lambda_2^p\right)^2}\left(\frac{Q}{\sqrt{\mu\varepsilon}L_1L_2}\right)^2 + \alpha\left(\lambda_1 - \lambda_1^p\right) \tag{5}$$

$$\alpha = \frac{KL_1}{\mu L_2 L_3}$$

where is a dimensionless ratio between the stiffness of the spring and that of the elastomer. Equation (5) shows that the axial force is balanced by contributions of three origins: the elasticity of the elastomer, the permittivity of the elastomer, and the elasticity of the spring. Equation (5) can also be obtained by invoking the Maxwell stress [15, 16].

Inserting (1) into (4), we obtain that

$$\frac{\Phi}{L_3}\sqrt{\frac{\varepsilon}{\mu}} = \frac{1}{\left(\lambda_1 \lambda_2^p\right)^2}\left(\frac{Q}{\sqrt{\mu\varepsilon}L_1 L_2}\right) \tag{6}$$

The actuator has three dimensionless parameters of design: the prestretches in the two directions in the plane of the elastomer, λ_1^p and λ_2^p, as well as the normalized stiffness of the spring α. These parameters of design are prescribed once the actuator is constructed.

Equations (5) and (6) are the equations of state, relating the dimensionless loading parameters, $P/\left(\mu L_2 L_3\right)$ and $\Phi/\left(L_3\sqrt{\mu/\varepsilon}\right)$, to the dimensionless generalized coordinates, λ_1 and $Q/\left(L_1 L_2\sqrt{\varepsilon\mu}\right)$.

These nonlinear equations of state can be displayed graphically on a plane spanned by the two dimensionless generalized coordinates as shown in Fig. 2. Plotted on this plane are the lines of constant force and the lines of constant voltage. Fig. 2 can be used to locate the state of the actuator under prescribed axial force and voltage. In plotting the equations of state in Fig. 2, we have set the parameters of design to a particular set of values.

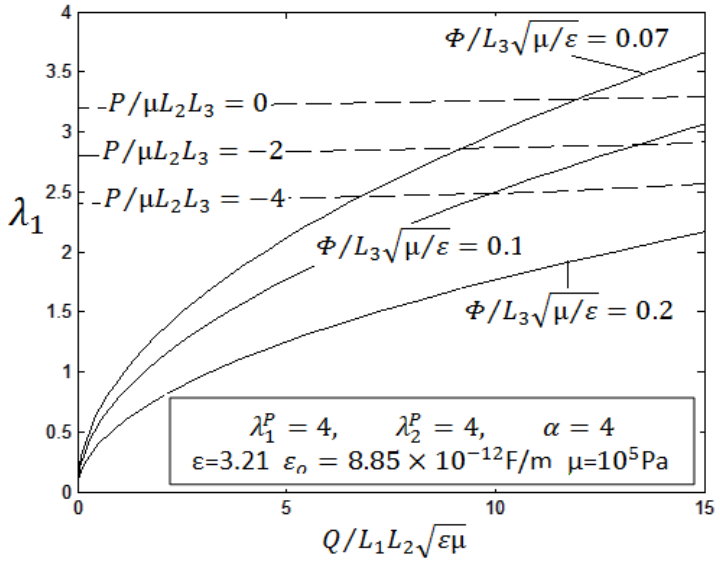

Fig. 2: A graphical representation of the equations of state.

When the design variables $(\alpha, \lambda_1^p, \lambda_2^p)$ are prescribed, the state of the actuator is characterized by two generalized coordinates: the stretch λ_1^p in the axial direction, and the charge Q on one of the electrode.

3. MODES OF FAILURE

The range of operation of an actuator is limited by various modes of failure. Each mode of failure restricts the state of the actuator to a region on the plane of the generalized coordinates. The common region that averts all modes of failure constitutes the set of allowable states. To illustrate the procedure to construct the region of allowable states, several representative modes of failure are considered [17, 18].

First electromechanical instability (EMI) of the elastomer is considered. As the applied voltage is increased, the elastomer reduces its thickness, so that the voltage induces a high electric field. The positive feedback between a thinner elastomer and a higher electric field may cause the elastomer to be reduced drastically, resulting in an electrical breakdown. This electromechanical instability can be analyzed by using a standard method in thermodynamics. [19].

Consider a three-dimensional space, with the generalized coordinates λ1 and Q being the horizontal axes, and the Helmholtz free energy A being the vertical axis. In this space, the free-energy function $A(\lambda_1, Q)$ is a surface. A point on the surface represents a state of the actuator, and a curve on the surface represents a path of actuation. Imagining a plane tangent to the surface at a state (λ_1, Q). The slopes of this tangent plane are PL1 and Φ, according to (3) and (4).

For a state (λ_1, Q) to be stable against arbitrary small perturbations in the generalized coordinates, the surface $A(\lambda_1, Q)$ must be convex at the point (λ_1, Q). This condition of stability is equivalent to the following set of inequalities:

$$\frac{\partial^2 A(\lambda_1, Q)}{\partial \lambda_1^2} > 0 \tag{7a}$$

$$\frac{\partial^2 A(\lambda_1, Q)}{\partial Q^2} > 0 \tag{7b}$$

$$\frac{\partial^2 A(\lambda_1, Q)}{\partial \lambda_1^2} \cdot \frac{\partial^2 A(\lambda_1, Q)}{\partial Q^2} > \left(\frac{\partial^2 A(\lambda_1, Q)}{\partial \lambda_1 \partial Q} \right)^2 \tag{7c}$$

Based on the three inequalities, (7a) ensures mechanical stability, (7b) electrical stability, and (7c) electromechanical stability. Using (1), it is noticeable that (7a) and (7b) are satisfied for all values of (λ_1, Q), but (7c) is violated for some values of (λ_1, Q). A combination of (1) and (7c) shows that the electromechanical instability sets when:

$$\frac{Q}{\sqrt{\mu\varepsilon} L_1 L_2} = \sqrt{(1+\alpha)\lambda_1^4 \left(\lambda_2^p\right)^2 + 3} \tag{8}$$

This equation corresponds to the curve marked by EMI in Fig. 3. The curve divides the (λ_1, Q) plane into two regions. Above the curve, the actuator is stable against small perturbation of the generalized coordinates. Below the curve, the actuator undergoes electromechanical instability.

The second mode of failure is the *electrical breakdown* (EB) of the elastomer. Even before the electromechanical instability sets, the electric field in the elastomer may become too high, leading to localized conduction path through the thickness of the elastomer. For the complexity of the microscopic process of electrical breakdown, it will not be addressed in this paper. To illustrate the procedure of design, we assume that electrical breakdown occurs when the true electric field exceeds a critical value *Ec*. For the ideal dielectric elastomer, $D = \varepsilon E$, where the true electric displacement is $D = Q/\lambda_1\lambda_2^p L_1 L_2$, the condition for electric breakdown is

$$\frac{Q}{\sqrt{\mu\varepsilon}L_1L_2} = \lambda_1\lambda_2^p E_C\sqrt{\frac{\varepsilon}{\mu}} \tag{9}$$

Equation (9) corresponds to the straight line marked by EB on the (λ_1, Q) plane as shown in Fig. 3. The actuator in a state in the region above this straight line will not suffer from the electrical breakdown.

Loss of tension of the elastomer when the voltage Φ is large is considered, or axial force *P* is compressive and of a large magnitude, the stress in the plane of the elastomer may cease to be tensile. This loss of tension will cause the elastomer to buckle out of the plane, so that elastomer will no longer generate force of actuation. To avert this mode of failure, the stress is required to be tensile in every direction in the plane of the elastomer. That is, both the stress along the axial direction and the stress in the circumferential direction are required to be tensile, $S_1 > 0$ and $S_2 > 0$. Following [20], the nominal stress in the axial direction is obtained in terms of the two generalized coordinates:

$$\frac{S_1}{\mu} = \left(\lambda_1 - \lambda_1^{-3}\left(\lambda_2^p\right)^{-2}\right) - \left(\frac{Q}{\sqrt{\mu\varepsilon}L_1L_2}\right)^2 \lambda_1^{-3}\left(\lambda_2^p\right)^{-2} \tag{10}$$

Setting the critical condition in (10), we obtain that

$$\frac{Q}{\sqrt{\mu\varepsilon}L_1L_2} = \sqrt{\lambda_1^4\left(\lambda_2^p\right)^2 - 1} \tag{10a}$$

Similarly, nominal stress s_2 in terms of the two generalized coordinates can be obtained:

$$\frac{S_2}{\mu} = \left(\lambda_2^p - \left(\lambda_2^p\right)^{-3}\lambda_1^{-2}\right) - \left(\frac{Q}{\sqrt{\mu\varepsilon}L_1L_2}\right)^2 \left(\lambda_2^p\right)^{-3}\lambda_1^{-2} \tag{11}$$

Setting the critical condition s_2=0 in (11), the following equation can be obtained:

$$\frac{Q}{\sqrt{\mu\varepsilon}L_1L_2} = \sqrt{\lambda_1^2\left(\lambda_2^p\right)^4 - 1} \tag{11a}$$

The critical conditions for loss of tension, s_1=0 and s_2=0, are plotted in Fig. 3. A comparison of (8) and (10a) shows that, for spring-roll actuators, loss of tension in

the axial direction will always precede electromechanical instability. In contrary, other types of dielectric elastomer actuators may fail by electromechanical instability [21, 22].

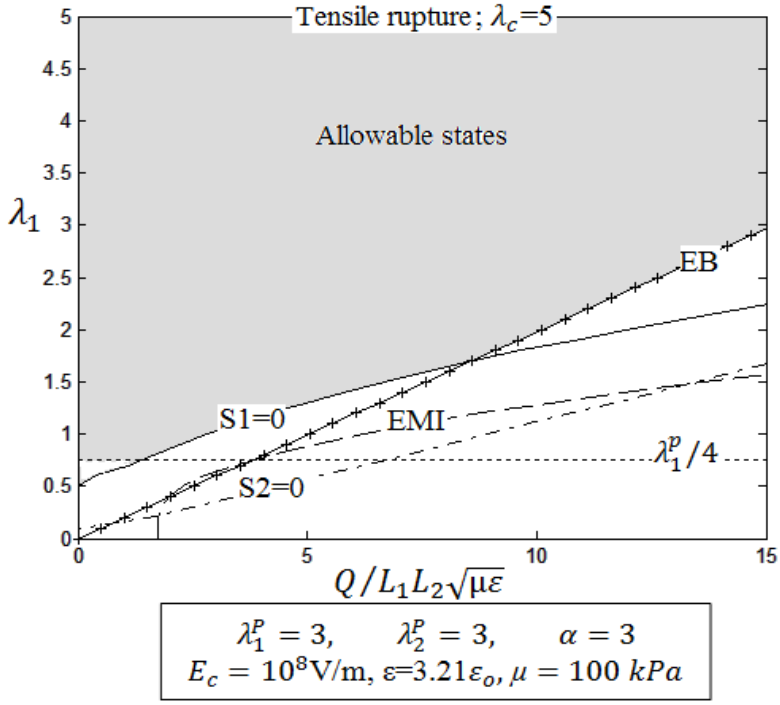

Fig. 3 A graphical representation of modes of failure

Next *tensile rupture* of the elastomer is considered. When an elastomer is stretched too severely, the elastomer may rupture. The critical condition for tensile rupture is not well quantified. Here the simple criterion that the elastomer will rupture when either stretch, λ_1 or λ_2 exceeds a critical value λ_c is used. A representative value λ_c = 5 is included in Fig.3.

The *compressive limit* of the spring is finally considered. The spring in the spring-roll actuator is designed to be under compression. When the spring is compressed excessively, however, it may deform plastically. The length of the spring at its relaxed state is $\lambda_1^p L_1$, and the length of the actuated spring is $\lambda_1 L_1$. We assume that the spring deforms plastically when λ_1^p / λ_1 exceeds a critical value *c*, which we set to be *c* = 4. In the (λ_1, Q) plane, Fig. 3, the region above the line $\lambda_1 = \lambda_1^p / c$ will guarantee that the spring remains elastic.

The modes of failure discussed in this section are all averted in the shaded region in Fig. 3. As evident from the above discussion, this region of allowable states will depend on the critical conditions for various modes of failure.

4. DESIGN OF A SPRING-ROLL DIELECTRIC ELASTOMER ACTUATOR

4.1 Actuation Range (Maximum and Minimum Required Actuation)

For maximum required actuation, as illustrated from fig. 4, moving from a lower state to an upper state along the applied voltage curve, the compressive axial force has to decrease in magnitude. That is, behind the point of intersection of the applied voltage curve and the prescribed axial force curve, the actuator becomes unable to burden the already prescribed compressive load which it designed for. Therefore, we should not move upwards on the applied voltage curve to surpass the point of maximum required actuation $\lambda_{1\,\max}$.

For minimum required actuation, to avoid actuation in the region of modes of failure, the actuator should work in the allowable states region; therefore the first point on the applied voltage curve in this region is the minimum required actuation. In other words, the lowest actuation of the applied voltage curve in the allowable state region is the minimum required actuation $\lambda_{1\,\min}$.

Actuation range = Maximum required actuation ($\lambda_{1\,\max}$) – Minimum required actuation ($\lambda_{1\,\min}$), (which is a dimensionless value).

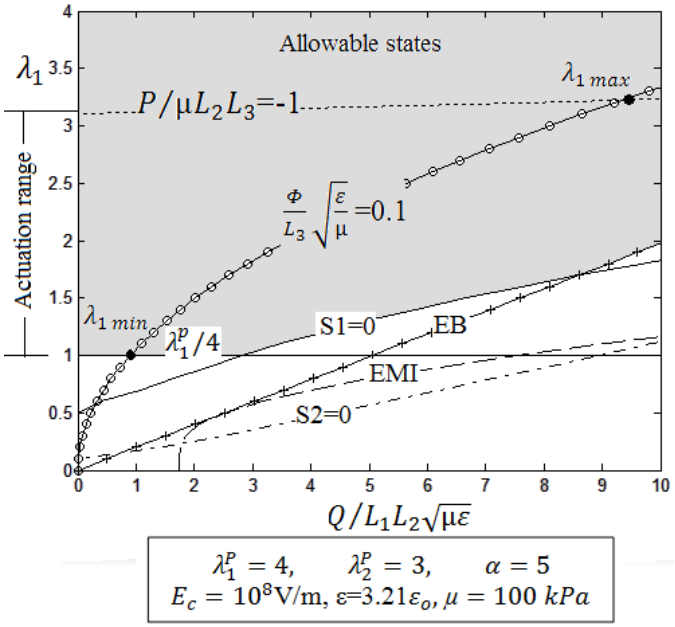

Fig. 4: Actuation range

4.2 Criteria for Designing Dielectric Elastomer Roll Actuator

1. The allowable states are upper bounded by tensile rupture $\lambda_C = 5$, and lower bounded by loss of tension $S_1 = 0$ and electrical breakdown EB.

2. Line of constant force should be located in the region of allowable states.
3. The actuator should be able to achieve both maximum and minimum actuation.
4. Physical dimensions of the actuator; actuator length $\lambda_1 L_1$, and actuator diameter D, have to fit the purpose it designed for.
5. The applied voltage should be regulated (stabilized) and controlled to a specific value.
6. Charges flow to the electrodes of the actuator should be controlled by a charge controller.

5. THE PARAMETERS OF THE DESIGN

Mickael Moscardo et al. [23], stated that "In the absence of the applied force $P/\mu L_2 L_3$, the combination of $\lambda_1^p = 1$, $\lambda_2^p = 5$ and α=0 gives the optimal range of actuation". This is not true because the curve of constant force according to these values is almost touch the curve of EMI, that is, it is not far from modes of failure and each of maximum actuation and maximum actuation range are not achieved at these values as it is clear in Fig. 5.

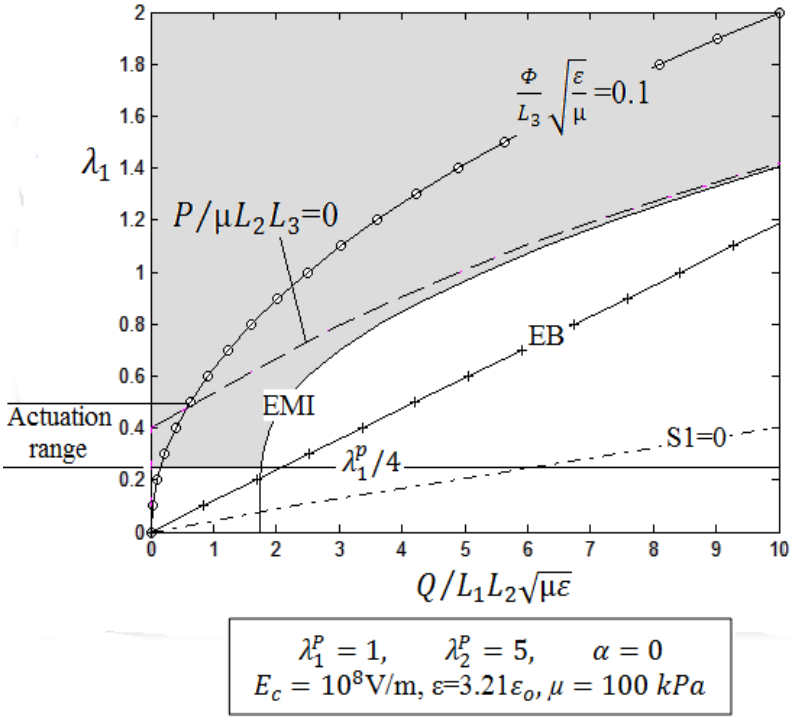

Fig. 5: Maximum actuation range are not achieved at $\lambda_1^p = 1$, $\lambda_2^p = 5$ and α=0

Maximum actuation is not also achieved at $\lambda_1^p = 2.85$, $\lambda_2^p = 5$ and α=2.5. In this case $\lambda_{1\max}$ will be 1.9 as shown in Fig. 6.

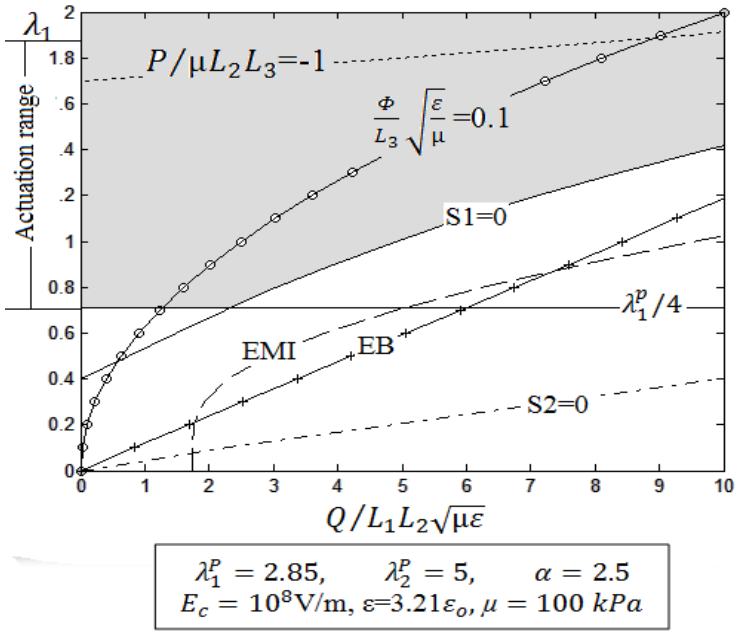

Fig. 6: Maximum actuation is not achieved at $\lambda_1^p = 2.85$, $\lambda_2^p = 5$ and α=2.5

Now we study the effect of parameters of design on the actuation. To gain insight into the behavior, we will now fix two of the three parameters of design $(\lambda_1^p, \lambda_2^p, and\ \alpha)$, and vary the third. P is not a design parameter but it is a given parameter. Figure 7 shows the effect of λ_1^p on the actuation at $\lambda_2^p = 2$, α=2 and $P/\mu L_2 L_3 = -1$. It is noticed that as λ_1^p increases, λ_1 increases and the highest actuation (optimal value) is achieved at $\lambda_1^p = 5$.

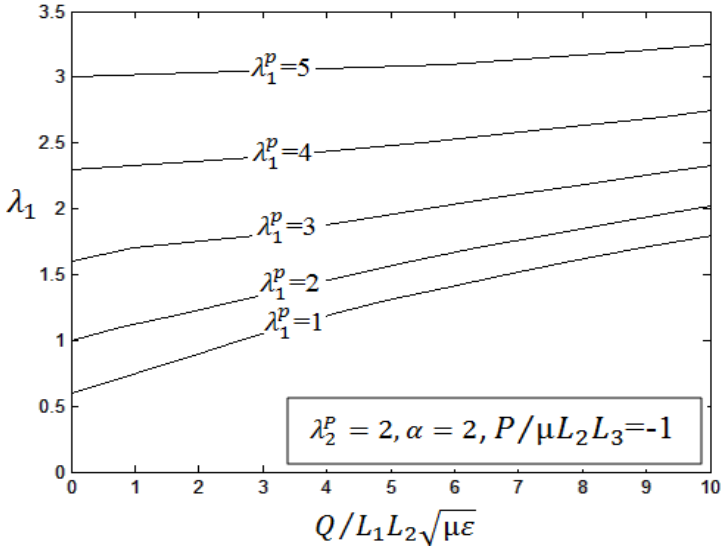

Fig. 7: The effect of λ_1^p on the actuation at $\lambda_2^p = 2$, α=2 and $P/\mu L_2 L_3 = -1$

We will now fix the values of λ_1^p , and α and vary λ_2^p . Fig. 8 shows the effect of λ_2^p on the actuation at $\lambda_1^p = 2$, α=2, and $P/\mu L_2 L_3 = -1$. It is noticed that as λ_2^p increases, λ_1 decreases and the highest actuation (optimal value) is achieved at $\lambda_2^p = 2$.

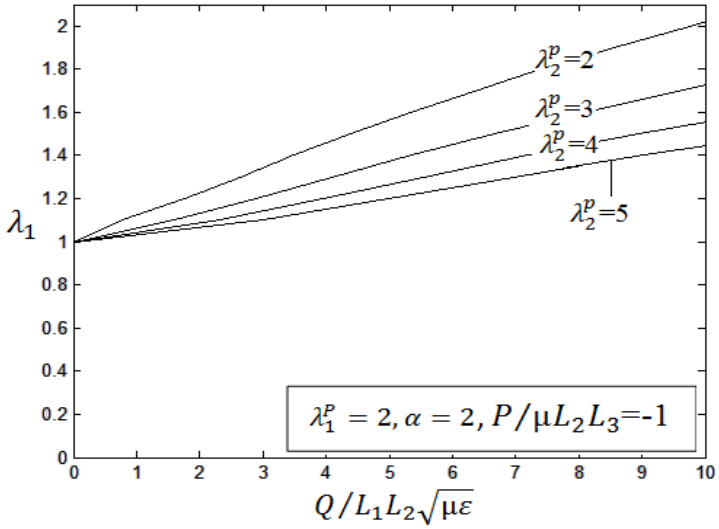

Fig. 8: The effect of λ_2^p on the actuation at $\lambda_1^p = 2$, α=2 and $P/\mu L_2 L_3 = -1$

We will now fix the values of λ_1^p , and λ_2^p and vary α. Fig. 9 shows the effect of α on the actuation at $\lambda_1^p = 2$, $\lambda_2^p = 2$ and $P/\mu L_2 L_3 = -1$. It is noticed that as α increases, λ_1 increases and the highest actuation (optimal value) is achieved at α=10.

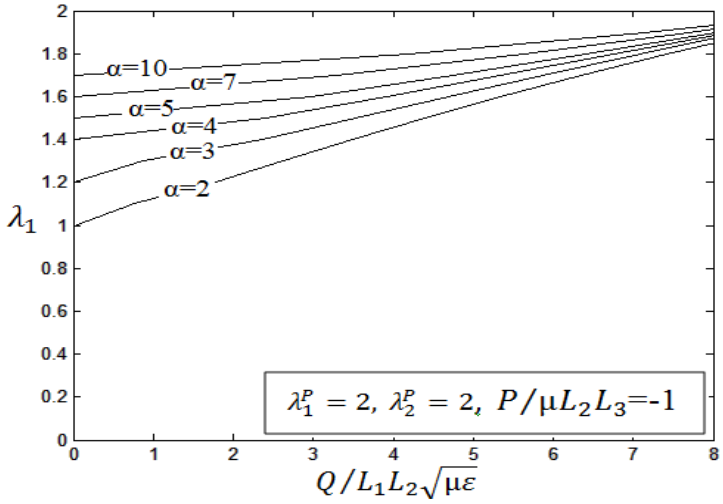

Fig. 9: The effect of α on the actuation at $\lambda_1^p = 2$, $\lambda_2^p = 2$ and $P/\mu L_2 L_3 = -1$

From the above curves, we can deduce that the optimal values of design parameters are: $\lambda_1^p = 5$, $\lambda_2^p = 2$; and α=10. These results can be verified by plotting the generalized coordinates λ_1 and $Q/\mu L_1 L_2 \sqrt{\mu\varepsilon}$ using different sets of design parameters.

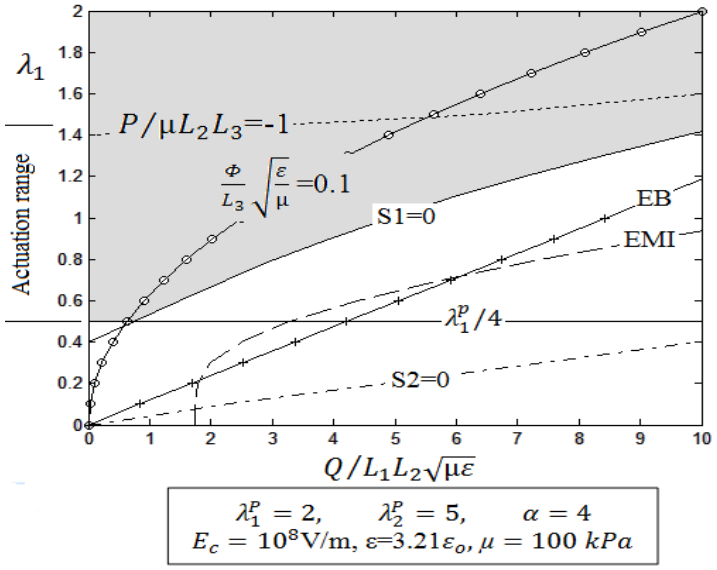

Fig. 10: Actuation at $\lambda_1^p = 2$, $\lambda_2^p = 5$, α=4, $P/\mu L_2 L_3 = -1$ and $\Phi/L_3\sqrt{\mu/\varepsilon} = 0.1$

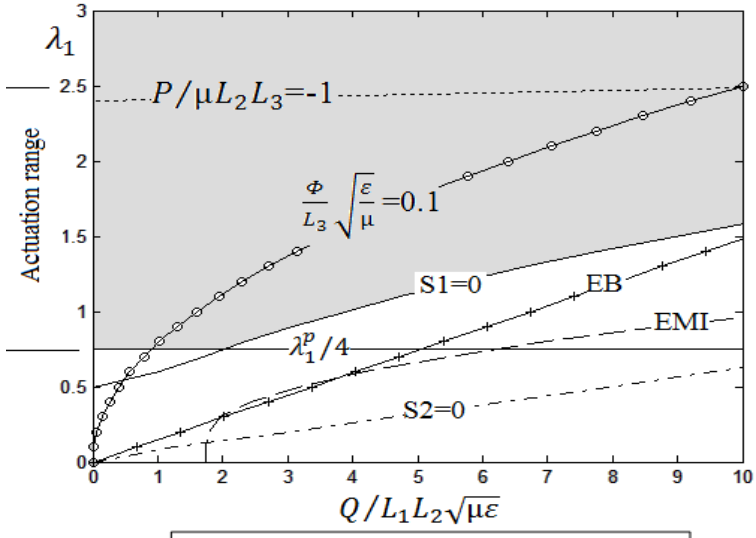

Fig. 11: Actuation at $\lambda_1^p = 3$, $\lambda_2^p = 4$, α=6, $P/\mu L_2 L_3 = -1$ and $\Phi/L_3\sqrt{\mu/\varepsilon} = 0.1$

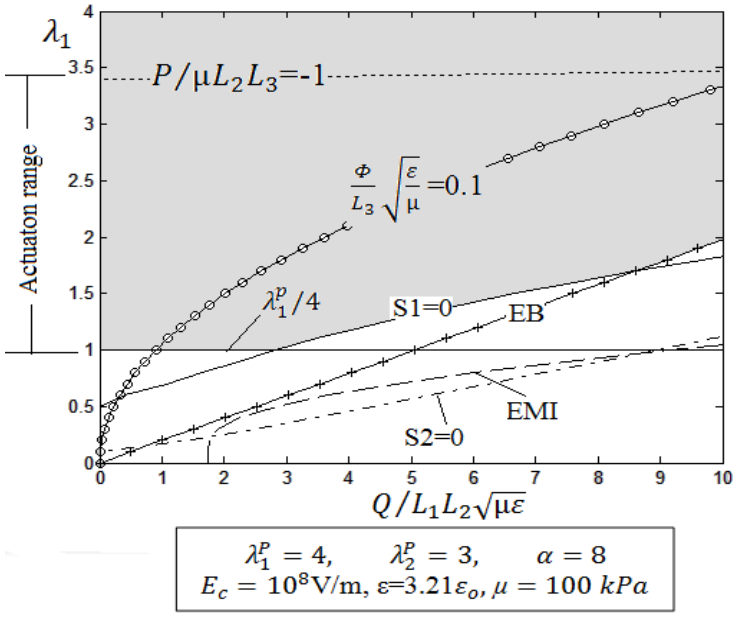

Fig. 12: Actuation at $\lambda_1^p = 4$, $\lambda_2^p = 3$, α=8, $P/\mu L_2 L_3 = -1$ and $\Phi/L_3\sqrt{\mu/\varepsilon} = 0.1$

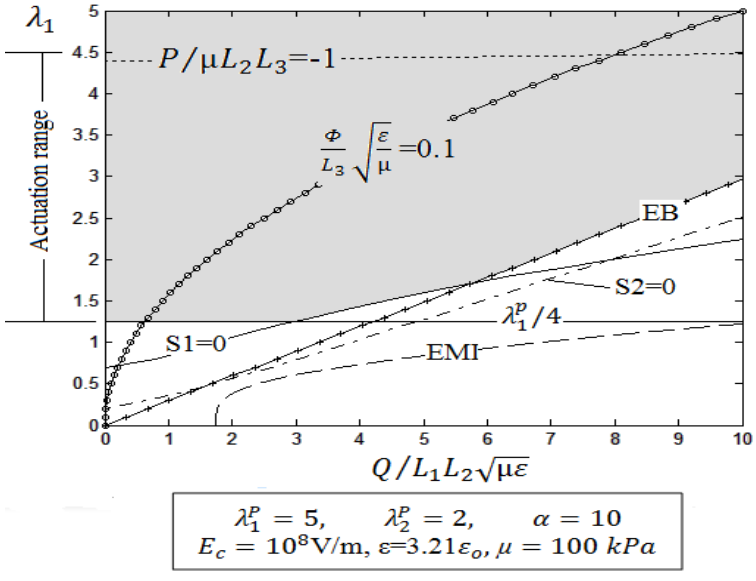

Fig. 13: Actuation at $\lambda_1^p = 5$, $\lambda_2^p = 2$, α=5, $P/\mu L_2 L_3 = -1$ and $\Phi/L_3\sqrt{\mu/\varepsilon} = 0.1$

Figures (7-13) prove that the maximum actuation is achieved using $\lambda_1^p = 5$, $\lambda_2^p = 2$ and α=10 (the optimal design parameters). At $\lambda_1^p = 5$, $\lambda_2^p = 2$ and α=10, maximum actuation range is also achieved, allowable states region widens, and region of modes of failure contracts.

The most common realistic values of stiffness k of music wire stainless steel spring are in the range from 20 to 2500. When α=10, the values of k are very huge and not realistic. To get realistic values for k the design parameter α=10 is changed in our design to be α=2. Then the realistic optimal design parameters will be $\lambda_1^p = 5$, $\lambda_2^p = 2$ and α=2.

6. DESIGN A SPRING-ROLL DIELECTRIC ELASTOMER ACTUATOR

After deriving the optimal values of design parameters λ_1^p, λ_2^p and α, the relaxed elastomer dimensions $\lambda_1^p L_1$, $\lambda_2^p L_2$ and $\lambda_3^p L_3$ should fit the purpose of the actuator designed for.

The value of L_3 affects the value of the dimensionless applied voltage $\Phi/L_3\sqrt{\mu/\varepsilon}$. L_2 *and* L_3 affect the value of the dimensionless axial force $P/\mu L_2 L_3$, while L_1, L_2, *and* L_3 affect the value of α, [$\alpha = (kL_1)/(\mu L_2 L_3)$]. The dimensionless applied voltage $\Phi/L_3\sqrt{\mu/\varepsilon}$ can take values from 0.04 to 0.4 however for actuator designing, it is better to take values between 0.05 and 0.1. The dimensionless axial force $P/\mu L_2 L_3$ can take values from 0 to -30, but for actuator designing it is better to take values between 0 and -10. It should not be positive otherwise changes from compressive to tensile force.

In appendix A, equations of state based Matlab software is developed to design Spring-Roll Dielectric Elastomer using the optimal design parameters $\lambda_1^p = 5$, $\lambda_2^p = 2$, α=2, the dielectric ε=3.21 for VHB 4910 material at frequency of 1k Hz, the permittivity $\varepsilon_o = 8.85\times10^{-12}$ Farad/ meter, the shear modulus of this material $\mu = 10^5$ Pascal. Samples of these designed items are mentioned in Table [1].

Table [1]: Actuator design and required specifications

Actuator designed specifications							**Actuator known specifications**	
Φ	L_3	$\frac{\Phi}{L_3}\sqrt{\frac{\varepsilon}{\mu}}$	L_2	$\frac{P}{\mu L_2 L_3}$	L_1	k	P	$L_{1\ relax}$
4000	0.001	0.071	0.1	0	0.02	950	0	0.1
4000	0.001	0.071	0.1	-1.0526	0.03	633	-10	0.15
4000	0.001	0.071	0.1	-2.1053	0.04	475	-20	0.2
4000	0.001	0.071	0.1	-3.1579	0.05	380	-30	0.25
4000	0.001	0.071	0.1	-4.2105	0.06	317	-40	0.3
4000	0.001	0.071	0.1	-5.2632	0.07	271	-50	0.35
4000	0.001	0.071	0.1	-6.3158	0.08	237.5	-60	0.4
4000	0.001	0.071	0.1	-7.3684	0.09	211	-70	0.45
4000	0.001	0.071	0.1	-8.4211	0.1	190	-80	0.5
4000	0.001	0.071	0.1	-9.4737	0.11	173	-90	0.55
4000	0.001	0.071	0.1	-9.5694	0.12	174	-100	0.6

Actuation and actuation range of the above designed actuators can be determined from the curves of the generalized coordinates which can be plotted using Matlab program which developed for this purpose, (appendix B). Table 2 summarizes the achieved results.

Table [2]: Maximum actuation and Actuation range

Maximum actuation	Actuation range		P	$\frac{P}{\mu L_2 L_3}$	Φ	$\frac{\Phi}{L_3}\sqrt{\frac{\varepsilon}{\mu}}$
	From	To				
3.358	1.25	3.358	0	0	4000	0.071
3.01	1.25	3.01	-10	-1.0526	4000	0.071
2.651	1.25	2.651	-20	-2.1053	4000	0.071
2.305	1.25	2.305	-30	-3.1579	4000	0.071
1.945	1.25	1.945	-40	-4.2105	4000	0.071
1.625	1.25	1.625	-50	-5.2632	4000	0.071
1.255	1.25	1.255	-60	-6.3158	4000	0.071

7. CONCLUSION

This paper described new techniques to design optimal parameters of dielectric elastomer spring–roll actuator. We introduced a new definition of actuation range concept. We considered maximum actuation and actuation range as measures of performance; on this basis, we deduced the values of optimal design parameters. The graphical representation of the equations of state proves the correct choice of values of optimal design parameters. Construction of actuator and modes of failure demonstrate the region of allowable states and define the conditions of robust design. We developed an optimal design parameters based Mat-Lab program to design details of the actuator; length, width and thickness of the dielectric elstomer laminate, applied voltage, stiffness of the spring, actuation and actuation range of the actuator. The achieved results confirmed the reliability and robustness of the proposed techniques.

8. REFERENCES

[1] Woosang JUNG, Yutaka TOI, "Computational Modeling of Electromechanical Behaviors of Dielectric Elastomer Actuators," Proceedings of International MultiConference of Engineers and Computer Scientists, volume III, March 17-19-2010 , IMECS(2010)

[2] Tianhu He, Xuanhe Zhao, and Zhigang Suo2, "Dielectric elastomer membranes undergoing inhomogeneous deformation," Journal of Applied Physics, 106, 083522 (2009).

[3] S. Rosset, P. Dubois, M. Niklaus, and H.R. Shea, "Large Stroke Miniaturized Dielectric Elastomer Actuators," IEEE, (2009).

[4] Ailish O'Halloran, Fergal O'Malley, and Peter McHugh, "A review on dielectric elastomer actuators, technology, applications, and challenges," JOURNAL OF APPLIED PHYSICS 104, 071101 (2008).

[5] Michael T. Petralia and Robert J. Wood, "Fabrication and analysis of dielectric-elastomer minimum-energy structures for highly-deformable soft robotic systems," The 2010 IEEE/RSJ International Conference on Intelligent Robots and Systems October 18-22, 2010, Taipei, Taiwanb (2010).
[6] Yanju Liu, Liwu Liu, Zhen Zhang and Jinsong Leng, "Dielectric elastomer film actuators: characterization, experiment and analysis," SMART MATERIALS AND STRUCTURES, 18 095024 (10pp) (2009).
[7] Rui Zhang, Patrick Lochmatter, Andreas Kun and Gabor Kovacs, "Spring Roll Dielectric Elastomer Actuators for a Portable Force Feedback Glove," Proceedings of SPIE Vol. 6168, 61681T, (2006).
[8] Q. Pei, R. Pelrine, S. Stanford, R. Kornbluh, M. Rosenthal, Synthetic Metals, 135-136, 129- 131(2003).
[9] Q. Pei, R. Pelrine, S. Stanford, R. Kornbluh, M. Rosenthal, K. Meijer, R. "Full, Smart Structures and Materials," Proc. of SPIE Vol. 4698, 246 (2002).
[10] Guggi Kofod, "The static actuation of dielectric elastomer actuators: how does pre-stretch improve actuation?," J. Physics. D: Appled Physics. 41 215405 (11pp) (2008)
[11] Woosang JUNG, Yutaka TOI, "Computational Modeling of Electromechanical Behaviors of Dielectric Elastomer Actuators," Proceedings of the International MultiConference of Engineers and Computer Scientists 2010 Vol III, IMECS 2010, March 17-19, 2010, Hong Kong.
[12] X. Zhao, W. Hong, Z. Suo, Physical review B 76 (2007).
[13] G. Kofod, M. Paajanen, S. Bauer, Applied Physics" a-Materials Science & Processing 85, 141(2006).
[14] Z. G. Suo, X. H. Zhao, and W. H. Greene, Journal of the Mechanics and Physics of Solids 56, 467-486 (2008).
[15] R. Zhang, P. Lochmatter, A. Kunz, G. Kovacs, Smart Structures and Materials, Proc. of SPIE Vol. 6168 (2006).
[16] G. Kovacs, P. Lochmatter, M. Wissler, Smart Materials and Structures, Vol. 16, S306-S317 (2007).
[17] R. E. Pelrine, R. D. Kornbluh, J. P. Joseph, Sensors and Actuators A 64, 77 (1998).
[18] J. S. Plante, S. Dubowsky, International Journal of Solids and Structures 43, 7727 (2006).
[19] A. N. Norris, Applied Physics Letters 92, 026101 (2008).
[20] X. Zhao, Z. Suo, Applied Physics Letters 91 (2007).
[21] Tianhu He, Xuanhe Zhao and Zhigang Suo, "Equilibrium and stability of dielectric elastomer membranes undergoing inhomogeneous deformation," School of Engineering and Applied Sciences, Harvard University, (2-10-2008).
[22] Christoph Keplinger, Martin Kaltenbrunner, Nikita Arnold, and Siegfried Bauer, Röntgen's electrode-free elastomer actuators without electromechanical pull-in instability,Applied physical science, (December 15, 2009).
[23] Mickael Moscardo, Xuanhe Zhao, Zhigang Suo,_ and Yuri Lapusta, "On designing dielectric elastomer actuators," Journal of Applied Physics 104, 093503, (2008).

9. APPENDICES

APPENDIX A

```
function [phi, l3, PHI, l2, axialforce, k, l1]=design (p, l1relax)
% l1: length of dielectric elastomer membrane before prestraining
% l2: width of dielectric elastomer membrane before prestraining
% l3: thickness of dielectric elastomer membrane before prestraining
% phi: applied voltage
% PHI: dimensionless applied voltage
% p: axial force
% axialforce: dimensionless axial force
% k: spring stiffness
% l1relax: axial length of the actuator after prestretching
% This program is used to design a Spring-Roll Dielectric Elastomeractuator
epselon=3.21*8.85*10.^-12;
mu=10.^5;
for phi=3000: 50: 4000
   for l3=7.5*10.^-4: 10.^-4: 10.^-3
      PHI=(phi/l3)*sqrt(epselon/mu);
      while PHI >=0.05 && PHI <=0.1
         disp(phi);
         disp (l3);
         disp (PHI);
         break;
      end
      for l2=0.1: 0.01: 1
         axialforce=p/(mu*l2*l3);
         if axialforce >= -10 && axialforce <= 0
            disp (l2);
            disp (axialforce);
            break;
         end
      end
   end
end
k=10*mu*l2*l3/l1relax;
l1=l1relax/5;
disp (l1);
disp (k);
```

APPENDIX B

```
function [q, d1]=draw (d1p, d2p, a, p, phi)
% q: dimensionless charge (the first generalized co-ordinate)
% d1p: lampda1p, prestrain of the length of the dielectric elastomer membrane
% d2p: lampda2p, prestrain of the width of the dielectric elastomer membrane
% a: alpha
% p: dimensionless axial force
% phi: dimensionless applied voltage
% d1: strain (the second generalized co-ordinate)
% This program is used to plot modes of failure, dimensionless axial force, and dimensionless
 % applied voltage
d1=[0: 0.1: 5];
q=sqrt(((1+a)*(d2p.^2)*(d1.^4)) +3);
plot(q, d1, 'b');
hold on
d1=[0: 0.1: 5];
q= 1.6855*d2p*d1;
plot(q, d1, 'k');
hold on
d1=[0: 0.1: 5];
q=sqrt(((d2p.^2)*(d1.^4)) -1);
plot(q, d1, 'm');
hold on
d1=[0: 0.1: 5];
q=sqrt((d2p.^4)*(d1.^2) -1);
plot(q, d1, 'g');
Hold on
d1=[0: 0.1: 5];
q=phi*(d2p.^2)*(d1.^2);
plot(q, d1, 'r');
hold on
d1=[0: 0.1: 5];
```

```
q=sqrt((d2p.^2 * d1.^4) -1 + (a * d2p.^2 * d1.^4) - (a * d1p * d2p.^2 * d1.^3) - (p * d2p.^2 * d1.^3));
plot(q, d1, 'c');
hold on
d1=0*q + d1p/4;
plot (q, d1, 'k')
```

الوصول بمعاملات تصميم مشغلات الإلاستومر العازل الملفوف على زنبرك إلى الحالة المثلى

يمكن تحسين أداء المشغلات الميكانيكية المصنوعة من الإلاستومر العازل الملفوف على زنبرك بشكل ملحوظ عن طريق الاختيار الحكيم لبارامترات تصميمه (أى المشغل).

ولكن هذا التصميم يواجه تحدياً للأسباب الآتية:

- عدم خطية المعادلات التى تصيغ التصميم.
- قد تتعرض هذه المشغلات لأنماط متعددة من الانهيار.
- صعوبة تحديد القيم المثلى لبارامترات التصميم.
- كيفية قياس أداء هذه المشغلات.

ولهذا النوع من المشغلات ثلاث بارامترات تصميم لابعدية (ليس لها وحدات قياس):

- مط أولى لرقاقة الإلاستومر فى اتجاه الطول.
- مط أولى لرقاقة الإلاستومر فى اتجاه العرض.
- النسبة بين صلابة الزنبرك وصلابة الإلاستومر

وتحدّد قيم هذه البارامترات قبل الإنتهاء من تشييد (تركيب) هذا النوع من المشغلات. ويهدف هذا البحث إلى الوصول إلى القيم المثلى لبارامترات تصميم مشغلات الإلاستومر العازل الملفوف على زنبرك حتى يمكن الوصول إلى أقصى استطالة.

وفى هذا البحث ايضاً تم استحداث برنامج سوفت وبير لتمثيل المعادلات التى تصيغ التصميم تمثيلاً بيانياً عند أي قيمة من قيم بارامترات التصميم وبرنامج آخر لتصميم ابعاد المشغل فى حالة الاسترخاء، وأيضاً الجهد المسلط عليه، و صلابة الزنبرك المستخدم فيه وذلك عند معرفة طول المشغل والحمل الواقع عليه. وقد أعدت جداول أدرج فيها عينات من هذه التصميمات عند أطوال مختلفة للمشغلات وعند عدد من الأحمال المختلفة الواقعة عليها، كما تم ايضاً إيجاد النهاية العظمى للاستطالة ومدى الاستطالة للتصميمات السابقة وتم إدراجها فى جدول آخر. ويصف هذا البحث كيفية تفادى منطقة الانهيارات والخروج منها.

وبمقارنة هذا البحث بالأعمال الموجودة حالياً نجد أن النتائج التى تحققت تؤكد تفوقه [1–6]. وبهذا يقدم هذه البحث تقنيات تصميم قوية وموثوق بها فى تصميم مشغلات الإلاستومر العازل الملفوف على زنبرك والتى تفوق استطالتهاعن 300% ويمكن استخدامها فى تطبيقات مختلفة فى الأغراض الطبية.